Study of the $e^+e^- \to D^{(*)+}D^{*-}$ process near the open charm threshold with initial state radiation

V. Zhukova
Belle Collaboration

Novosibirsk, 19 March

Spectrum of charmonium

- Vector states above open-charm threshold are not fully understood
- Parameters of ψ states obtained from $\sigma_{\text{tot}}(e^+e^- \to \text{hadrons})$
  - are model-dependent
  - have large uncertainties
- Data collected should allow for coupled-channel analysis

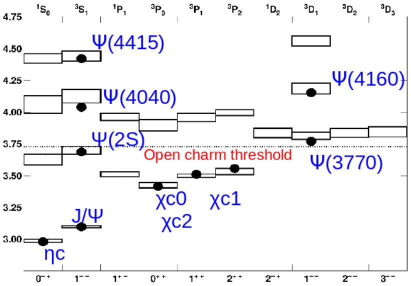

Spectrum of charmonium

- Vector states above open-charm threshold are not fully understood
- Parameters of ψ states obtained from $\sigma_{\text{tot}}(e^+e^- \to \text{hadrons})$
  - are model-dependent
  - have large uncertainties
- Data collected should allow for coupled-channel analysis

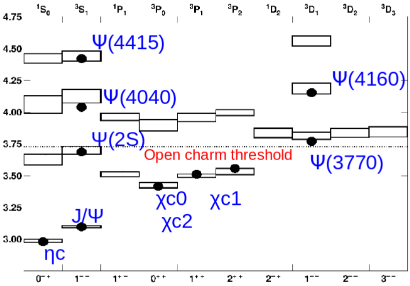

Solution $\Longrightarrow$ Measure exclusive cross sections

Comparison with previous results

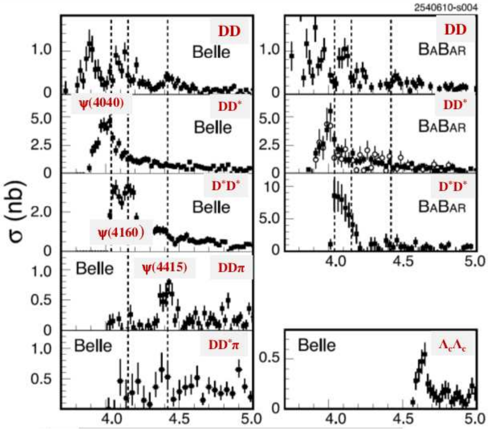

- Belle and BaBar results agree with each other
- Statistics is too low to study the structure of the cross sections
- Sum of all measured excusive cross-section to open-charm channels saturates the total cross section

Comparison with previous results

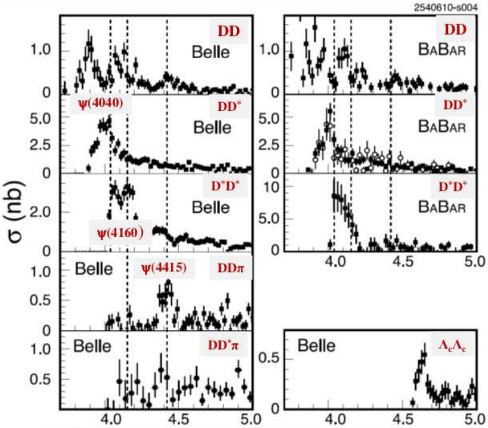

- Belle and BaBar results agree with each other
- Statistics is too low to study the structure of the cross sections
- Sum of all measured excusive cross-section to open-charm channels saturates the total cross section

Goals:

- To improve accuracy of cross section measurements
- To measure separately cross sections for all 3 possible helicity combinations (TT, LT, LL) for the $D^*\bar{D}^*$ final state

Method

- Partial reconstruction
- Reconstruct $\mathbf{D}^*$, γ_{ISR}

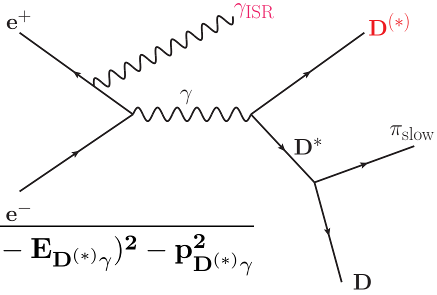

$$\mathbf{M}_{\mathsf{recoil}}(\mathbf{D}^{(*)}\gamma) = \sqrt{(\mathbf{E}_{\mathbf{c.m.}} - \mathbf{E}_{\mathbf{D}^{(*)}\gamma})^{\mathbf{2}} - \mathbf{p}^{\mathbf{2}}_{\mathbf{D}^{(*)}\gamma}}$$

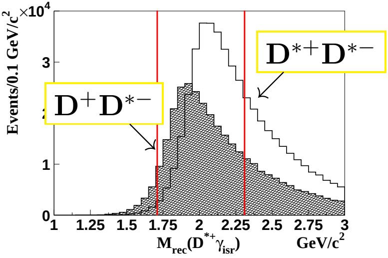

Method

- Partial reconstruction
- Reconstruct $\mathbf{D}^*$, γ_{ISR}

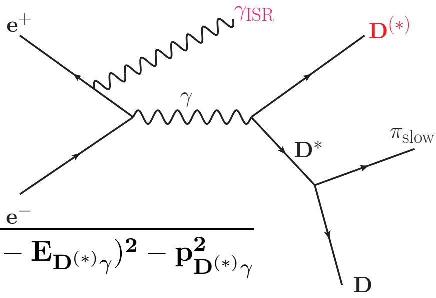

$$M_{\mathsf{recoil}}(\mathbf{D}^{(*)}\gamma) = \sqrt{(\mathbf{E_{c.m.}} - \mathbf{E_{D^{(*)}\gamma}})^2 - \mathbf{p^2_{D^{(*)}\gamma}}}$$

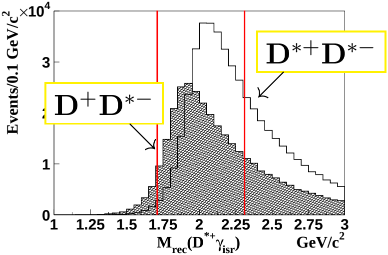

Problem: Cannot distinguish between $\mathbf{D}$, $\mathbf{D}^*$ and $\mathbf{D}^{**}$ in the final state

Method

- Partial reconstruction
- Reconstruct $\mathbf{D}^*$, γ_{ISR} and $\pi_{\mathbf{slow}}$

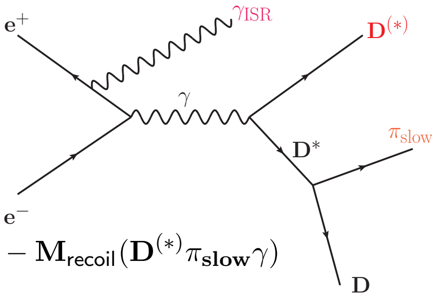

$$\Delta \mathbf{M}_{\text{recoil}} = \mathbf{M}_{\text{recoil}}(\mathbf{D}^{(*)}\gamma_{\text{ISR}}) - \mathbf{M}_{\text{recoil}}(\mathbf{D}^{(*)}\pi_{\mathbf{slow}}\gamma)$$

$\mathbf{e^+e^- \to D^+D^{*-}}$

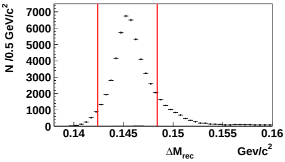

Recoil mass difference $\Delta \mathbf{M}_{\text{recoil}}$

↙ ↘

cut:

$\pm 3 MeV/c^2$

$\mathbf{e^+e^- \to D^{*+}D^{*-}}$

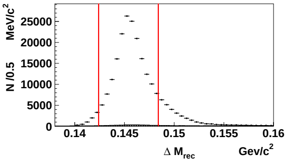

Method

- Partial reconstruction
- Reconstruct $\mathbf{D}^*$, γ_{ISR} and $\pi_{\mathbf{slow}}$
- $\mathbf{M}(\mathbf{D}^{(*)+}\mathbf{D}^{*-}) \equiv \mathbf{M}_{\text{recoil}}(\gamma_{\text{ISR}})$

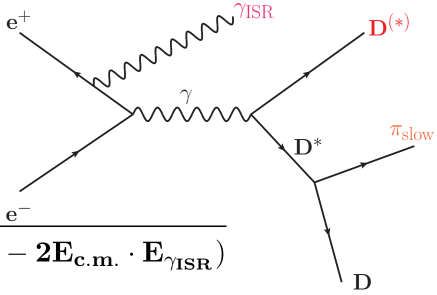

$$\mathbf{M}_{\text{recoil}}(\gamma_{\text{ISR}}) = \sqrt{(\mathbf{E}^2_{\mathbf{c.m.}} - \mathbf{2E}_{\mathbf{c.m.}} \cdot \mathbf{E}_{\gamma_{\mathbf{ISR}}})}$$

Refit $M_{\text{recoil}}(D^{(*)}\gamma_{\text{ISR}})$ to D^* mass to improve the $M_{\text{recoil}}(\gamma_{\text{ISR}})$ resolution

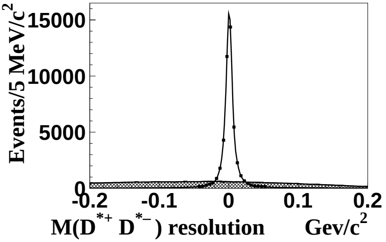

$\mathbf{M}_{\text{recoil}}(\gamma_{\text{ISR}})$ resolution:

Before re-fit — hatched histogram
After re-fit — solid line

Comparison with previous analysis

- Increased data sample: 547 $\mathrm{fb}^{-1} \Longrightarrow$ 951 fb^{-1}

- Additional modes for D reconstruction $\Longrightarrow$ $\mathbf{D^0}$ decay channels:

  1. $K^-\pi^+$
  2. K^-K^+
  3. $K^-\pi^-\pi^+\pi^+$
  4. $K^0_S\pi^+\pi^-$
  5. $K^-\pi^+\pi^0$
  6. $K^0_S K^+ K^-$
  7. $K^0_S\pi^0$
  8. $K^-K^+\pi^-\pi^+$
  9. $K^0_S\pi^+\pi^-\pi^0$

- Extended signal region for $M_{\text{recoil}}(D^{(*)}\gamma_{\text{ISR}})$

$$|(M_{\text{recoil}}(D^{(*)+}\gamma_{\text{ISR}}) - M(D^{*-}))| < \sout{200}\ 300\ \text{MeV}/c^2$$

- $$\sigma[e^+e^- \to D^{(*)+}D^{*-}] = \frac{dN/dM}{\eta_{\text{tot}}(M)\cdot dL/dM}$$

  dL/dM up to second-order QED corrections

  (Kuraev & Fadin (1985))

Backgrounds

1. Combinatorial background under the reconstructed $D^{(*)+}$ peak
2. Real $D^{(*)+}$ mesons and a combinatorial π_{slow}
3. Both the $D^{(*)+}$ meson and π_{slow} are combinatorial
4. Reflections from the processes $e^+e^- \to D^{(*)+}D^{*-}\pi^0\gamma_{\text{ISR}}$ where the π^0 is lost
5. Contribution of the $e^+e^- \to D^{(*)+}D^{*-}\pi^0_{\text{fast}}$ where the hard π^0_{fast} is misidentified as γ_{ISR}

Background contribution estimated from the data

Combinatorial backgrounds

$\mathbf{e^+e^- \to D^{*+}D^{*-}}$

$$M_{\text{bg (1)-(3)}} = 0.58 \cdot M_{\text{sb B}} + 0.53 \cdot M_{\text{sb C}} - 0.307 \cdot M_{\text{sb D}}$$

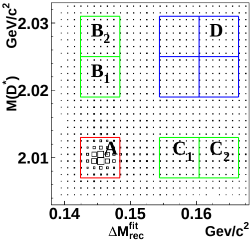

$\mathbf{e^+e^- \to D^{+}D^{*-}}$

$$M_{\text{bg (1)-(3)}} = 0.5 \cdot M_{\text{sb B}} + 0.43 \cdot M_{\text{sb C}} - 0.215 \cdot M_{\text{sb D}}$$

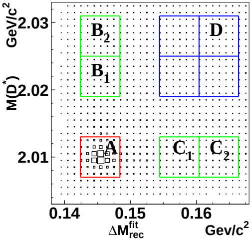

Backgrounds

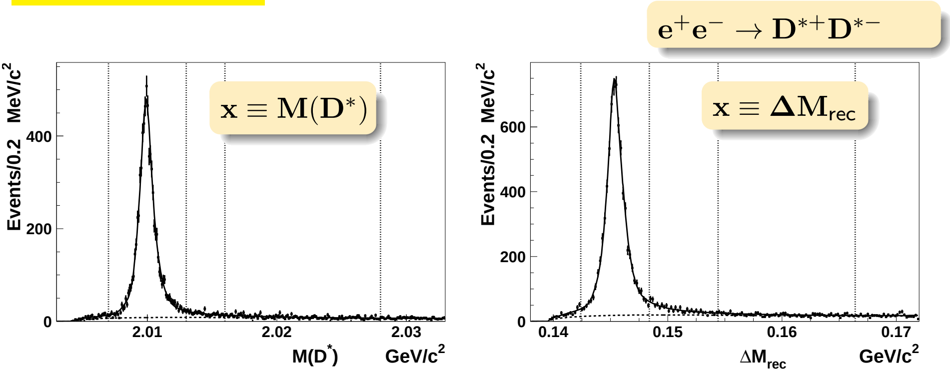

$$f = f_{\text{signal}} + f_{\text{background}}$$

$$f_{\text{background}} = \alpha \cdot \sqrt{x} \cdot (1 + \beta \cdot x + \gamma \cdot x^2)$$

$$M_{\text{bg (1)-(3)}} = 0.58 \cdot M_{\text{sb B}} + 0.53 \cdot M_{\text{sb C}} - 0.307 \cdot M_{\text{sb D}}$$

Backgrounds

$e^+e^- \to D^+D^{*-}$

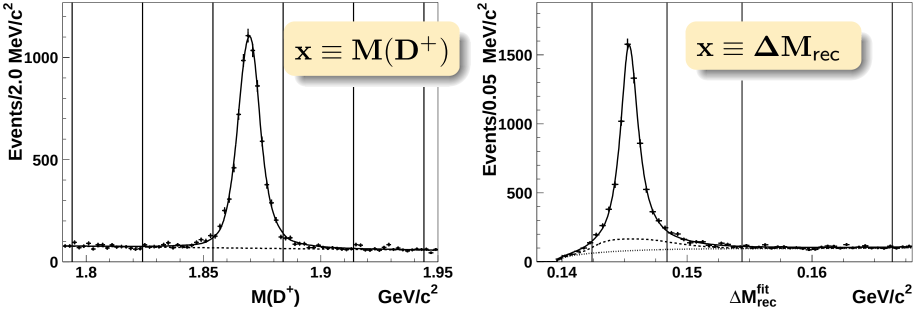

$$f = f_{\text{signal}} + f_{\text{background}}$$

$$f_{\text{background}} = \alpha \cdot \sqrt{x} \cdot (1 + \beta \cdot x + \gamma \cdot x^2)$$

$$M_{\text{bg (1)-(3)}} = 0.5 \cdot M_{\text{sb B}} + 0.43 \cdot M_{\text{sb C}} - 0.215 \cdot M_{\text{sb D}}$$

Mass spectra

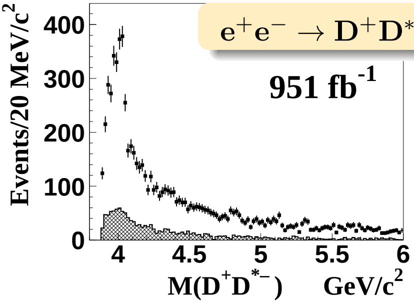

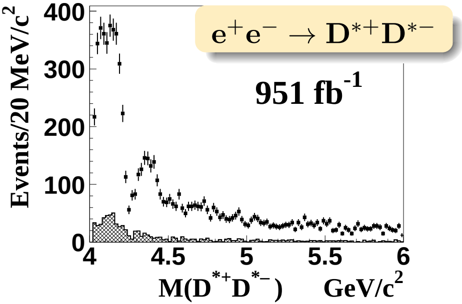

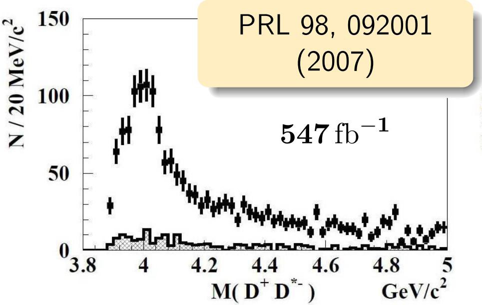

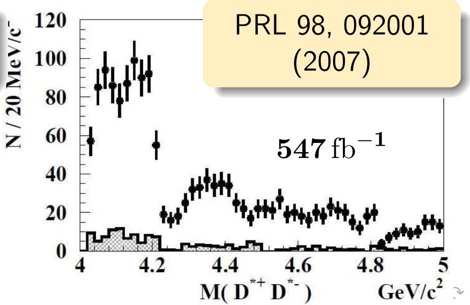

Reflection from the processes $e^+e^- \to D^{(*)+}D^{*-}\pi^0\gamma_{ISR}$

$e^+e^- \to D^+D^{*-}$

$e^+e^- \to D^{*+}D^{*-}$

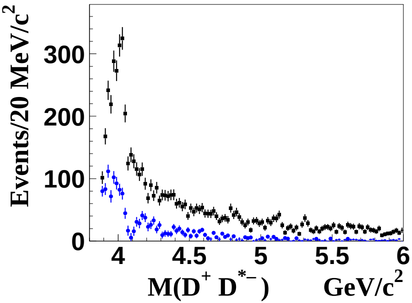

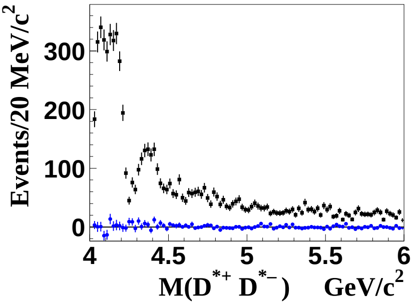

Background (blue points) from

$$e^+e^- \to D^{(*)+}D^{*-}\pi^0_{\text{miss}}\gamma_{\text{ISR}}$$

is evaluated from the isospin-conjugated process

$$e^+e^- \to D^{(*)0}D^{*-}\pi^+_{\text{miss}}\gamma_{\text{ISR}}$$

with the reconstruction of $D^{(*)0}$, π^-_{slow} and γ_{ISR}

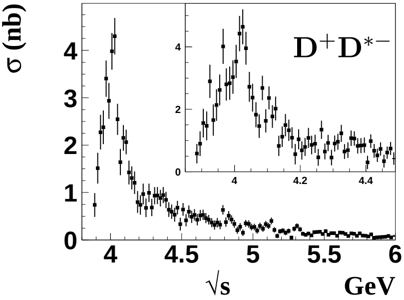
σ (nb)
D^+D^{*-}
√s
GeV

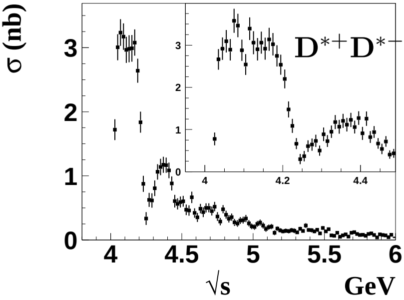
σ (nb)
$D^{*+}D^{*-}$
√s
GeV

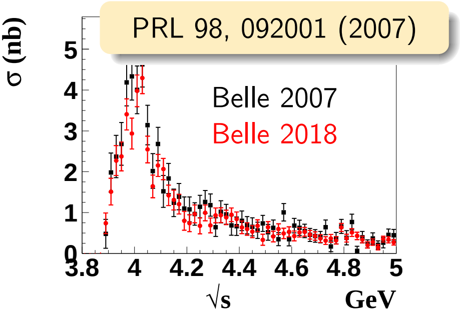
PRL 98, 092001 (2007)
σ (nb)
Belle 2007
Belle 2018
√s
GeV

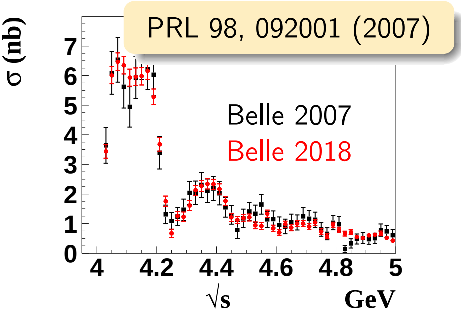
PRL 98, 092001 (2007)
σ (nb)
Belle 2007
Belle 2018
√s
GeV

Belle vs. BaBar

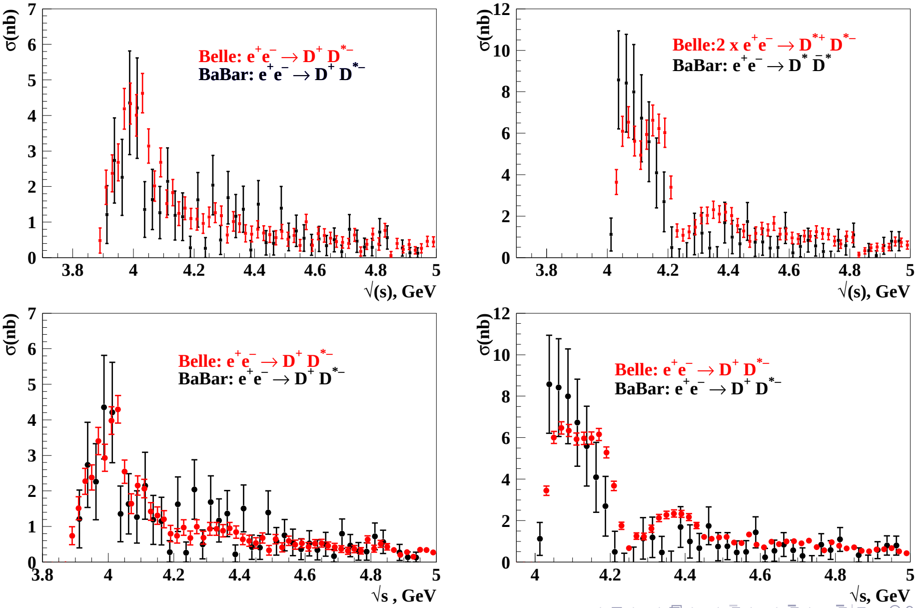

Angular analysis of the process $e^+e^- \to D^+D^{*-}$

- Study D^* helicity angle distribution in each bin of $M(D^+D^{*-})$
- D^* are transversely polarized $\Longrightarrow$ Check method

$4.05 < M(D^+D^{*-}) < 4.3\mathrm{GeV}/c^2$

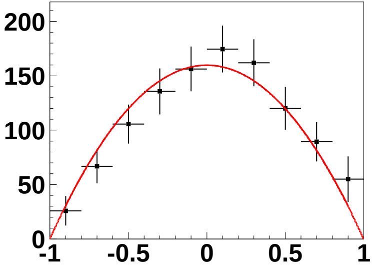

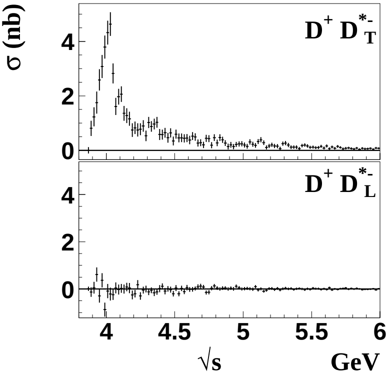

$$f_L = \sigma_L \cdot \cos^2\theta$$
$$f_T = \sigma_T \cdot (1 - \cos^2\theta)$$

$$F(\cos\theta) = \eta(\cos\theta)\cdot dM/dL\cdot(f_L + f_T)$$

Angular analysis of the process $e^+e^- \to D^{*+}D^{*-}$

- Study of the D^* helicity angle distribution in each bin of $M(D^{*+}D^{*-})$
- Helicity composition of the $D^{*+}D^{*-}$ final state:

$$\mathbf{D}^{*+}_{\mathrm{T}}\mathbf{D}^{*-}_{\mathrm{T}},\ \mathbf{D}^{*+}_{\mathrm{T}}\mathbf{D}^{*-}_{\mathrm{L}} \text{ and } \mathbf{D}^{*+}_{\mathrm{L}}\mathbf{D}^{*-}_{\mathrm{L}}$$

  - $D^*_{\mathrm{T}} \equiv$ transversely polarized D^* meson
  - $D^*_{\mathrm{L}} \equiv$ longitudinally polarized D^* meson

- Total cross section

$$\sigma = \sigma_{\mathrm{TT}} + \sigma_{\mathrm{TL}} + \sigma_{\mathrm{LL}}$$

$$f = \eta(c_1, c_2) \cdot dL/dM \cdot (f_{LL} + f_{TL} + f_{TT}) + f_{\mathrm{bg}}$$

$$c_1 \equiv \cos\theta_f \qquad c_2 \equiv \cos\theta_p$$

θ's are D^*'s helicity angles

$$f_{TT} = \sigma_{TT} \cdot (1 - c_1^2) \cdot (1 - c_2^2)$$
$$f_{TL} = \sigma_{TL} \cdot \left((1 - c_1^2) \cdot c_2^2 + c_1^2 \cdot (1 - c_2^2)\right)$$
$$f_{LL} = \sigma_{LL} \cdot c_1^2 \cdot c_2^2$$

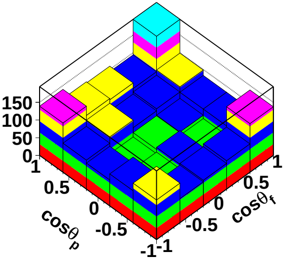

Fit results

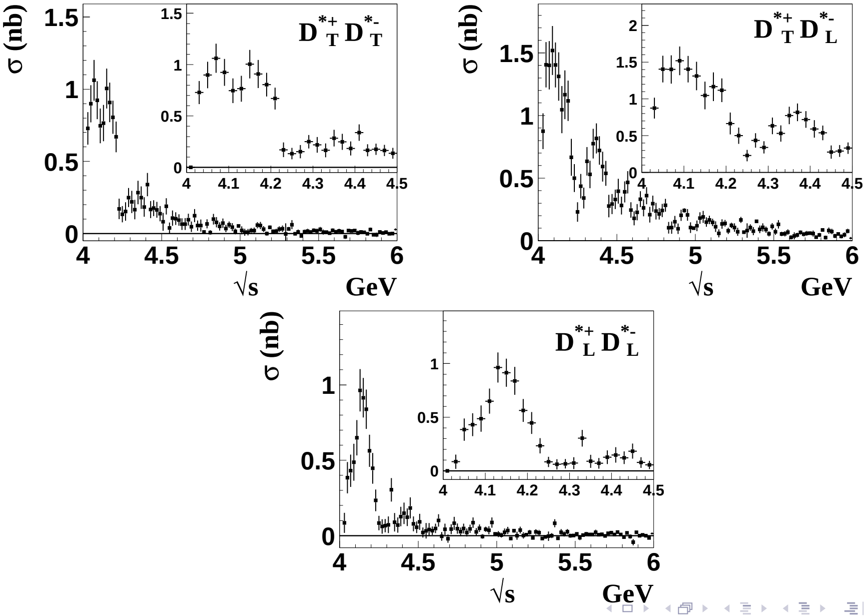

Conclusions

- We measured the exclusive cross sections of the $e^+e^- \to D^+D^{*-}$ and $e^+e^- \to D^{*+}D^{*-}$ processes
- The accuracy of the cross section measurements is increased
- The systematic uncertainties are significantly reduced
- For the $e^+e^- \to D^{*+}D^{*-}$ process we measured separately the cross sections for all three possible helicity final states (TT, LT and LL)

Conclusions

- We measured the exclusive cross sections of the $e^+e^- \to D^+D^{*-}$ and $e^+e^- \to D^{*+}D^{*-}$ processes
- The accuracy of the cross section measurements is increased
- The systematic uncertainties are significantly reduced
- For the $e^+e^- \to D^{*+}D^{*-}$ process we measured separately the cross sections for all three possible helicity final states (TT, LT and LL)

Thank you for your attention!

Criteria

- $|dr| < 2\,\mathrm{cm}$ and $|dz| < 4\,\mathrm{cm}$
- $\mathcal{P}_{K/\pi} = \mathcal{L}_K/(\mathcal{L}_K + \mathcal{L}_\pi) > 0.6$

$\mathbf{K_S}$ candidates:

- $|M_{inv}(\pi^+\pi^-) - M_{K^0_S}| < 15$ MeV/c^2
- the distance between the two pion tracks $< 1\,\mathrm{cm}$
- the transverse flight distance from IP $> 0.1\,\mathrm{cm}$
- the angle between the K_S momentum direction and decay path in $x - y$ plane $< 0.1\,\mathrm{rad}$

π_0 candidates:

- $|M_{inv}(\gamma\gamma) - M_{\pi_0}| < 15$ MeV/c^2

D^0 decay channels:

1. $K^-\pi^+$
2. K^-K^+
3. $K^-\pi^-\pi^+\pi^+$
4. $K^0_S\pi^+\pi^-$
5. $K^-\pi^+\pi^0$
6. $K^0_S K^+K^-$
7. $K^0_S\pi^0$
8. $K^-K^+\pi^-\pi^+$
9. $K^0_S\pi^+\pi^-\pi^0$

D^+ decay channels:

1. $K^+\pi^-\pi^-$
2. $K^0_S\pi^-$
3. $K^0_S K^+$

D^* decay channels:

1. $D^0\pi^+$

Analysis of the process $e^+e^- \to D^{(*)+}D^{*-}$

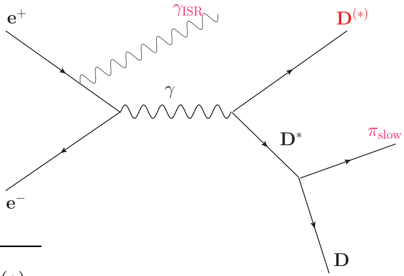

Method:

- partial reconstruction;
- reconstruction $\mathbf{D}^*$, $\pi_{\mathbf{slow}}$ and γ_{ISR};

$$M_{\text{recoil}}(D^{(*)}\gamma) = \sqrt{(E_{c.m.} - E_{D^{(*)}\gamma})^2 - p^2_{D^{(*)}\gamma}}$$

$$\Delta M_{\text{recoil}} = M_{\text{recoil}}(D^{(*)}\gamma_{\text{ISR}}) - M_{\text{recoil}}(D^{(*)}\pi_{slow}\gamma)$$

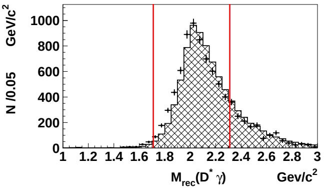

Spectrum of $M_{\text{recoil}}(D^*\gamma_{\text{ISR}})$

$$M_{\text{recoil}}(D^{(*)}\gamma) = \sqrt{(E_{c.m.} - E_{D^{(*)}\gamma})^2 - p^2_{D^{(*)}\gamma}}$$

Correction of γ_{ISR} energy

reference channel

$$e^+e^- \to \psi(2S)\gamma_{\text{ISR}}$$
$$\searrow$$
$$\psi(2S) \to J/\psi\pi^+\pi^-$$

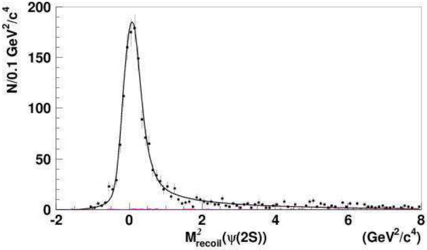

Conclusions:

phokhara generator describes the second radiation correction correctly

The same process on the other side

The recoil mass $\mathbf{M}_{\text{recoil}}(\mathbf{J}/\psi\pi^+\pi^-)$

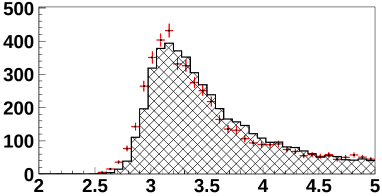

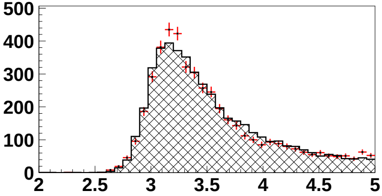

The recoil mass $M_{\text{recoil}}(D^*\gamma_{\text{ISR}})$

before correction γ_{ISR} energy

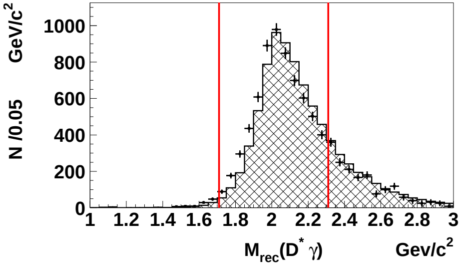

after correction γ_{ISR} energy

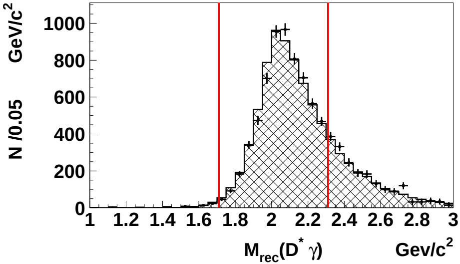

cut:

$$|M_{\text{recoil}}(D^*\gamma_{\text{ISR}}) - M(D^*)| < 300 MeV/c^2$$

Backgrounds

1. Combinatorial background under the reconstructed $D^{(*)+}$ peak
2. Real $D^{(*)+}$ mesons and a combinatorial π_{slow}
3. Both the $D^{(*)+}$ meson and π_{slow} are combinatorial
4. Reflections from the processes $e^+e^- \to D^{(*)+}D^{*-}\pi^0\gamma_{\text{ISR}}$ where the π^0 is lost
5. Contribution of the $e^+e^- \to D^{(*)+}D^{*-}\pi^0_{\text{fast}}$ where the hard π^0_{fast} is misidentified as γ_{ISR}

$\mathbf{e^+e^- \to D^+D^{*-}}$

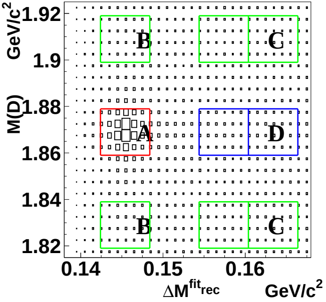

$\mathbf{e^+e^- \to D^{*+}D^{*-}}$

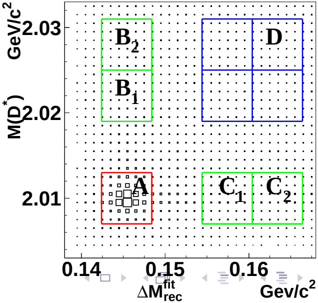

Cross sections calculation

$e^+e^- \to D^+D^{*-}$

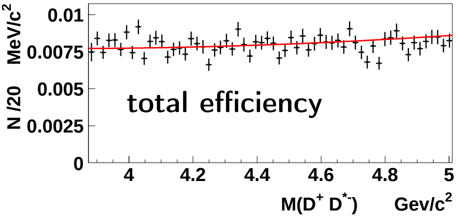

$e^+e^- \to D^{*+}D^{*-}$

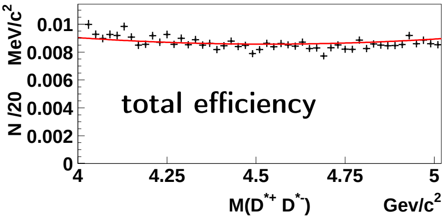

$$\sigma_{e^+e^- \to D^{(*)+}D^{*-}} = \frac{dN/dM}{\eta_{tot}(M)\cdot dL/dM}$$

dN/dM - mass spectrum,

η_{tot} - total efficiency,

dL/dM - differential luminosity;

$4.0 < M(D^{*+}D^{*-}) < 4.1\mathrm{GeV}/c^2$

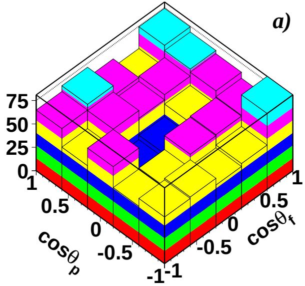

$4.1 < M(D^{*+}D^{*-}) < 4.25\mathrm{GeV}/c^2$

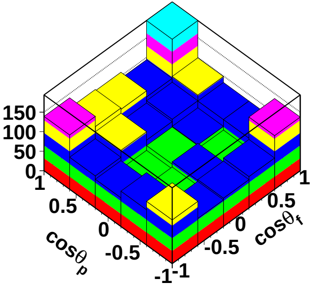

$4.25 < M(D^{*+}D^{*-}) < 4.6\mathrm{GeV}/c^2$

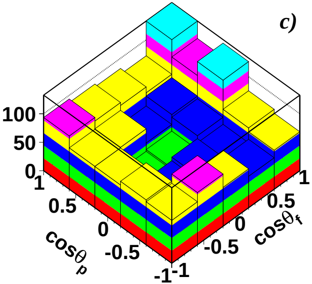

$M(D^{*+}D^{*-}) > 4.6\mathrm{GeV}/c^2$

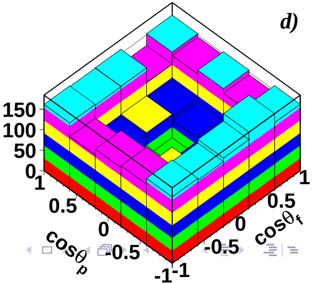

The summary of the systematic errors in the cross section calculation.

Source	D^+D^{*-}	$D^{*+}D^{*-}$
Background subtraction	2%	2%
Reconstruction	3%	4%
Selection	1%	1%
Angular distribution	–	2%
Cross section calculation	1.5%	1.5%
$\mathcal{B}(D^{(*)})$	2%	3%
MC statistics	1%	2%
Total	5%	7%